3D-Pharmacophore Models for Selective A_{2A} and A_{2B} Adenosine Receptor Antagonists

Jing Wei,[†] Songqing Wang,[†] Shaofen Gao,[‡] Xuedong Dai,[§] and Qingzhi Gao*[,§]

School of Pharmaceutical Science and Technology, Tianjin University, 92 Weijin Road, Nankai District, Tianjin 300072, P.R. China, NuBlocks LLC, 2420 Grand Avenue B1, Vista, California 92081, and Chemistry Department, XenoPort, Inc., 3410 Central Expressway, Santa Clara, California 95051

Received September 20, 2006

Three-dimensional pharmacophore models were generated for A_{2A} and A_{2B} adenosine receptors (ARs) based on highly selective A_{2A} and A_{2B} antagonists using the Catalyst program. The best pharmacophore model for selective A_{2A} antagonists (Hypo-A_{2A}) was obtained through a careful validation process. Four features contained in Hypo-A_{2A} (one ring aromatic feature (**R**), one positively ionizable feature (**P**), one hydrogen bond acceptor lipid feature (**L**), and one hydrophobic feature (**H**)) seem to be essential for antagonists in terms of binding activity and A_{2A} AR selectivity. The best pharmacophore model for selective A_{2B} antagonists (Hypo-A_{2B}) was elaborated by modifying the Catalyst common features (HipHop) hypotheses generated from the selective A_{2B} antagonists training set. Hypo-A_{2B} also consists of four features: one ring aromatic feature (**R**), one hydrophobic aliphatic feature (**Z**), and two hydrogen bond acceptor lipid features (**L**). All features play an important role in A_{2B} AR binding affinity and are essential for A_{2B} selectivity. Both A_{2A} and A_{2B} pharmacophore models have been validated toward a wide set of test molecules containing structurally diverse selective antagonists of all AR subtypes. They are capable of identifying correspondingly high potent antagonists and differentiating antagonists between subtypes. The results of our study will act as a valuable tool for retrieving structurally diverse compounds with desired biological activities and designing novel selective adenosine receptor ligands.

INTRODUCTION

Adenosine receptors belong to the superfamily of G-protein-coupled receptors (GPCRs). They were divided into four subtypes (A_1, A_{2A}, A_{2B}, and A_3) and have been cloned and characterized.[1] Adenosine receptors show a ubiquitous distribution in most mammal and human tissues and mediate many biological effects. It is well-known that A_{2A} and A_{2B} receptors can activate adenylate cyclase, while A_1 and A_3 receptors cause inhibition of the lyase.[2,3]

Stimulation of A_{2A} AR was found to reduce the binding affinity of dopamine D_2 receptors[4,5] and associate with the inhibition of tumor necrosis factor-α, IL-6, and IL-8.[6] Therefore, selective ligands of A_{2A} AR are currently of great interest as targets for therapeutic intervention, in particular for the treatment of Parkinson's disease. Recent studies have also demonstrated that A_{2A} receptor-stimulated adenylyl cyclase is aberrantly increased in cells expressing mutant huntingtin, and selective A_{2A} receptor antagonists retain their ability to revert A_{2A}-stimulated cyclic AMP formation in huntingtin-expressing cells.[7]

Activation of A_{2B} AR seemed to be involved in inducing IgE synthesis in mast cells,[8] the regulation of vascular smooth muscle tone,[9] cell growth,[10] intestinal function,[11] and modulation of neurosecretion.[12] Therefore, ligands of A_{2B} AR usually were considered a target for potential treatment of asthma and other serious disorders.

Since early times, the alkylxanthine derivative theophylline and its closely related analogue caffeine have been used clinically as antiasthmatic agents based on their weak adenosine antagonistic activity,[13] but their uses are associated with unpleasant side effects, such as insomnia and diuresis.[14] Recently, use of these drugs for relief of asthma has been supplanted by other classes, such as corticosteroids or β2-adrenergic agonists.[15] Studies on the mechanism of the side effects of xanthine type bronchodilators and the effect of another alkylxanthine clinical drug, enprofylline, suggested that the selectivity of adenosine antagonists for the A_{2B} adenosine subtype may play a very important role in their potential use as antiasthmatic agents.[16]

Over the past decade, a number of synthetic agonists and antagonists of the A_{2A} and A_{2B} ARs have been proposed, and some structure−activity relationship (SAR) studies have been reported.[2,17] It is known that all A_{2A} and A_{2B} AR antagonists are divided into xanthine and non-xanthine heterocyclic derivatives. A major problem of xanthine A_{2A} antagonists was their low-selectivity and low-water solubility.[18−20] As a result, non-xanthine type heterocyclic A_{2A} antagonists have been developed, and two main classes of bicyclic and tricyclic derivatives show interesting properties over xanthine derivatives.[21−24]

The study of the A_{2B} receptor lags behind those of other subtypes, mainly due to the lack of highly potent and selective pharmacological probes for this subtype.[25−27] Since Jacobson first published the 8-phenylxanthine carboxylic congener as a highly potent and selective antagonist for the human A_{2B} AR in 2000,[28] a series of 1,8-disubstituted xanthine derivatives was demonstrated to be potent A_{2B} AR

* Corresponding author phone: (408)616-7356; fax: (408)616-7210; e-mail: qgao@xenoport.com.
† Tianjin University.
‡ NuBlocks LLC.
§ XenoPort, Inc.

10.1021/ci600410m CCC: $37.00
Published on Web 03/02/2007

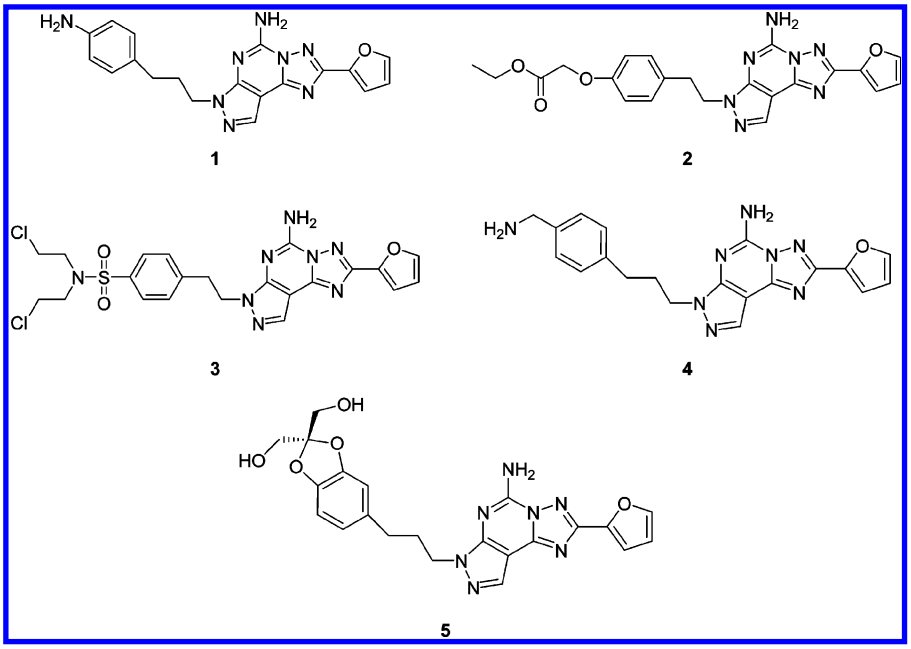

Figure 1. Structures of selective A_{2A} antagonists for the HipHop training set.

antagonists.[29−31] However, only a small number of nonxanthine derivatives have been reported as selective A_{2B} AR antagonistic compounds.[32−34]

Like other GPCR receptor families, adenosine receptors are transmembrane proteins. Such macromolecules are not easily crystallized for structural analysis by X-ray crystallography. For this reason, 3D pharmacophore models from the ligand-based approach are very useful for analyzing the ligand−receptor interactions.

Our current program focuses on the design and development of highly A_{2A}/A_{2B} selective adenosine receptor antagonists. To this end, we prefer to perform a systematic comparison of the pharmacophore models of the different AR subtypes in order to find the selective 3D pharmacophore for rational design and screening of A_{2A}/A_{2B} AR antagonistic ligands.

A powerful tool, widely used in ligand-based approach and rational drug design, is the common features hypothesis generation program, called HipHop, within the Catalyst software package.[35] The Catalyst package version 4.10 provides four methods of automatic generation of chemical feature-based pharmacophore models: two qualitative modules (HipHop and HipHopRefine) and two quantitative modules (HypoGen and HypoRefine). The HipHop algorithm finds the chemical features shared by a set of active compounds that seem commonly important for receptor interaction and then provides the compounds' relative alignments with a hypothesis expressing common features in 3D space. The generated 3D pharmacophore models can be useful for rational design and identifying novel active compounds through a database search. In the past years many successful applications in medicinal chemistry clearly demonstrate the usefulness of this ligand-based computational program.[36]

This paper presents the first study using a ligand-based computational approach to generate specific 3D pharmacophoric hypotheses for A_{2A} and A_{2B} adenosine receptors from their selective antagonists. All generated models have been validated using a wide test set of molecules containing structurally diverse selective antagonists for all subtypes of adenosine receptors ($A_1/A_{2A}/A_{2B}/A_3$). The pharmacophore models from this study can be used as a computational tool to design selective A_{2A}/A_{2B} AR antagonistic ligands.

Table 1. A_{2A} Training Set: Binding Affinities K_i (nM) and Selectivities for the Adenosine Receptors

		binding affinities K_i (nM)				selectivities		
no.	ref	A_1	A_{2A}	A_{2B}	A_3	A_1/A_{2A}	A_{2B}/A_{2A}	A_3/A_{2A}
1	21	2160	0.22	>10000	>10000	9818	>45455	>45455
2	21	4197	0.43	>10000	>10000	9760	>23256	>23256
3	21	5297	0.59	>10000	>10000	8978	>16949	>16949
4	21	576	0.13	>10000	>10000	4431	>76923	>76923
5	21	432	0.19	>10000	>10000	2274	>52632	>52632

MATERIALS AND METHODS

Training Set Selection. Based on the published literature, we collected a series of compounds as training sets to generate pharmacophore models for A_{2A} and A_{2B} antagonists according to their receptor-binding activity and selectivity.

In order to generate A_{2A} pharmacophore hypotheses, five A_{2A} selective antagonists were selected from the series of compounds that Schering-Plough is evaluating as potential clinical candidates for Parkinson's disease (compounds **1**−**5**, Figure 1).[21] These A_{2A} selective antagonists had high binding affinity with K_i values ranging from 0.13 to 0.59 nM, high selectivities with a K_iA_1/K_iA_{2A} ratio ranging from 2000 to 9000, and K_iA_{2B}/K_iA_{2A} and K_iA_3/K_iA_{2A} ratios greater than 10 000 as all compounds had no detectable affinity to subtype A_{2B} or A_3 (Table 1).

To generate A_{2B} pharmacophore hypotheses, five A_{2B} selective antagonists (compounds **6**−**10**, Figure 2) were chosen as the training set. The K_i value of binding affinity to A_{2B} AR ranged from 1.4 nM to 12 nM, and the K_i ratio toward other AR subtype were as follows: K_iA_{2A}/K_iA_{2B}, from 81 to 255; K_iA_1/K_iA_{2B}, from 36 to 205; and K_iA_3/K_iA_{2B}, from 83 to 289 (Table 2). Since there have been only a limited

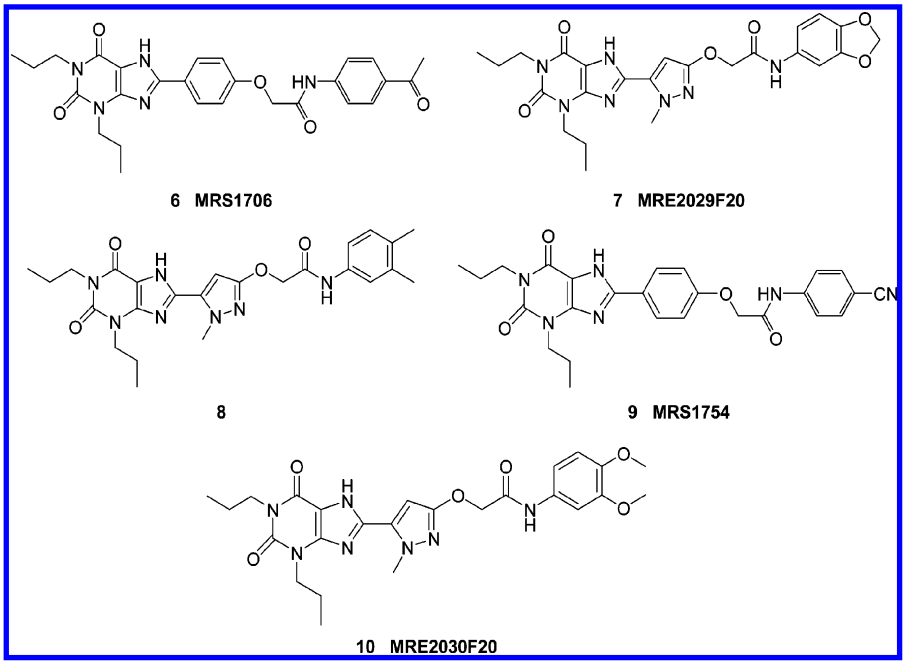

Figure 2. Structures of selective A_{2B} antagonists for the HipHop training set.

Table 2. A_{2B} Training Set: Binding Affinities K_i (nM) and Selectivities for the Adenosine Receptors

		binding affinities K_i (nM)				selectivities		
no.	ref	A_1	A_{2A}	A_{2B}	A_3	A_1/A_{2B}	A_{2A}/A_{2B}	A_3/A_{2B}
6	28	157	112	1.39	230	113	81	165
7	31	200	>1000	5.5	>1000	36	>182	>182
8	31	700	>1000	10	>1000	70	>100	>100
9	28	403	503	1.97	570	205	255	289
10	31	>1000	>1000	12	>1000	>83	>83	>83

number of highly selective A_{2B} antagonists developed during the past 10 years, the training and test sets we collected in this study consisted of the best antagonists in terms of the A_{2B} specificity.

Conformational Analysis. As the first step, all structures are built using a 2D/3D editor-sketcher and are minimized to a local energy minimum using the CHARMm-like force field implemented within the Catalyst software package.[35] Then Catalyst can generate a conformational model for each training set molecule that represents its flexibility. The conformational model thus generated consists of a representative set of conformers taken from a range of energetically reasonable conformations of a selected molecule. The conformational model will be used not only in hypothesis generation but also for fitting the compound to a hypothesis and for estimating the activity of the compound. Catalyst provides two types of conformational analysis: fast analysis and best quality analysis. Both methods were implemented using the Poling algorithm[37] to search for a set of representative conformers for each compound and automatically build only as many conformers as required for adequate coverage, up to a user-specifiable maximum. Fast conformational analysis is the method of choice for database generation, because the tolerances in a database query can be adjusted to minimize the effect of incomplete conformational coverage. Best quality conformational analysis is the method of choice if the conformational models are to be used for hypothesis generation. In this study, the best quality conformational analysis was applied to compounds in all training and test sets. For some compounds having stereogenic centers in the training or test sets, no experimental data on the biologically relevant conformations were available. Therefore, these compounds were arbitrarily assigned the "undefined" chirality, allowing the conformational analysis to create conformers so that the most appropriate configuration can be used to generate pharmacophore models and to perform fitting analysis. In this work, the best-quality conformer generation method was set at 250, the maximum number, with an energy range of 15 kcal/mol above the estimated global minimum for each molecule.

Generation of Pharmacophore Models. Catalyst uses chemical features that are not an atomistic description of the compound but a description of chemical properties (e.g., hydrogen bond donor or acceptor, etc.) to build up the pharmacophores. A pharmacophore model or hypothesis, as defined within the Catalyst package, is a collection of chemical features placed in 3D space that represent the most important characteristics of a ligand to bind to its receptor or have a certain biological affinity. Common features hypotheses generated by the HipHop algorithm in this work are designed specifically for finding the chemical features shared by a set of selective AR antagonists and for providing the compounds' relative alignments with a particular common features hypothesis.

At the beginning of the hypothesis generation, Catalyst examines every conformer of each training set molecule for the presence of chemical functions which will be selected and used to build the pharmacophore hypotheses. The common features hypothesis generation process then takes into account these chemical functions of the training set molecules and finds the 3D arrangement of chemical features common to all that are relevant to adenosine receptor interaction, thus generating a "HipHop model" corresponding to the training set antagonists and the receptor subtype.

Based on the feature characteristic of the training set molecules analyzed with Catalyst, the following chemical functions were selected from the feature dictionary of

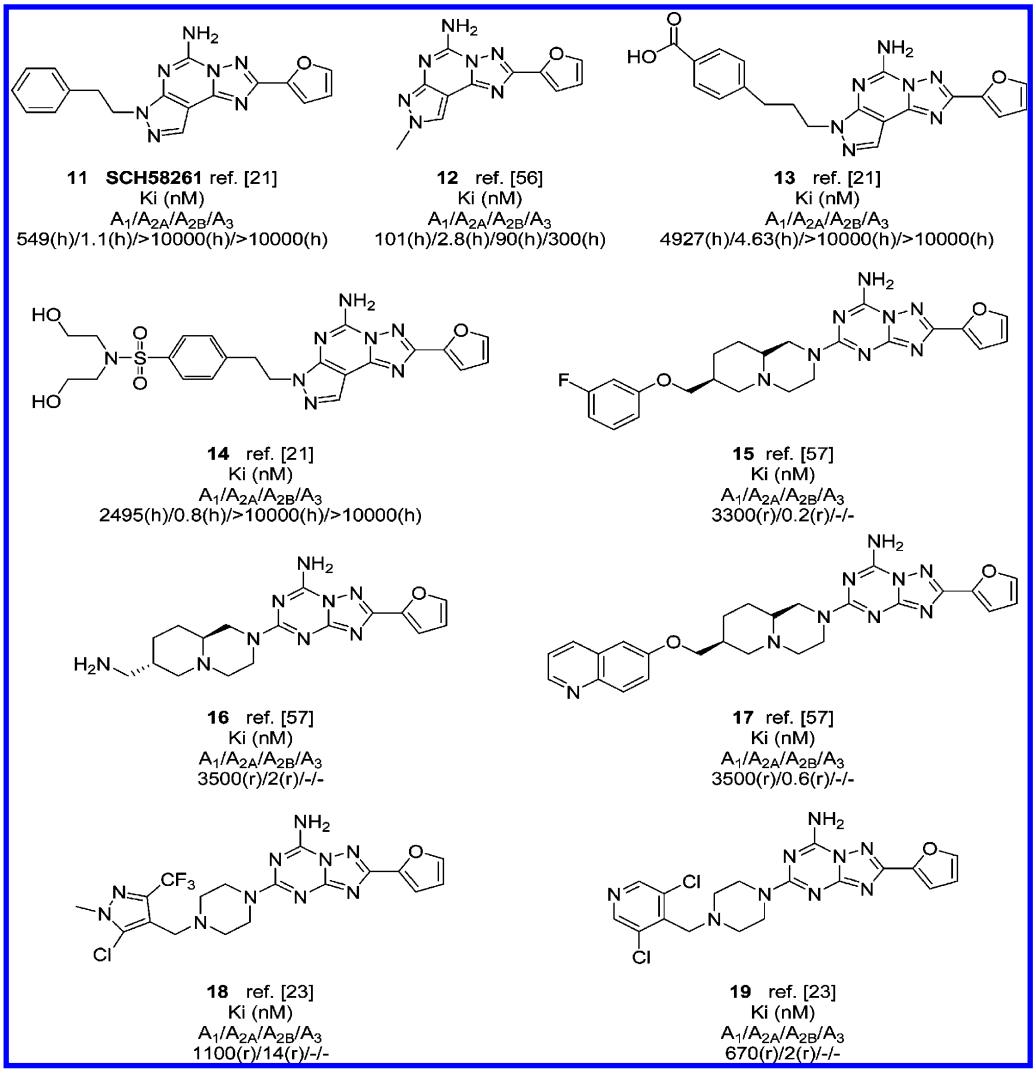

Figure 3. Test set of A_{2A} selective antagonists.

Catalyst for pharmacophore model generation: the hydrogen bond acceptor lipid (**L**), the ring aromatic (**R**), the hydrophobic (**H**), and the positively ionizable (**P**) for A_{2A} antagonist and **L**, **R**, and the hydrophobic aliphatic (**Z**) for A_{2B} antagonist. We selected the **L** feature over the hydrogen bond acceptor (**HBA**) feature because **L** includes basic nitrogen atoms not considered as the "hydrogen bond acceptor" by the definition of **HBA**.

Since the K_i values of the molecules in both training sets are within the nanomolar range and highly selective toward A_{2A} and A_{2B} adenosine receptors, all compounds were considered to contain equally important common features for the receptor binding as well as for the differentiation between the two subtypes. With this in mind, we set the "principal number" to 2 in order to ensure that all chemical features in the compounds would be considered when building the hypothesis space. Also, we set the "maximum omitting features" at 0 to force the mapping of all features for all compounds. All other parameters remained at their default settings.

After automatic hypothesis generation, ten common features hypotheses with ranking scores were selected by the HipHop program. The ranking score for each individual hypothesis was calculated by the program based on a ranking formula and the default definition of the "FIT" of a molecule to the hypothesis,[35] in order to determine the probability that a selected hypothesis mapped with the training set molecule by a chance correlation. The higher the score, the less likely it is that the molecule in the training set fit the hypothesis by a chance correlation.

Selection of the Best Pharmacophore Models. The following outlines our basic strategy in selecting best models for A_{2A} and A_{2B} antagonists from the generated hypotheses:

First, we performed a clustering analysis to categorize the obtained pharmacophoric models into several clusters. Unlike the conventional method that uses only the hypothesis with the highest ranking score as the candidate to evaluate the robustness against test sets, we argue that by further grouping the ten models into several clusters, based on their ranking scores and composition similarities, we can select pharmacophore models with more diversity built in for the evaluation process.

Second, we selected the top-ranking models from each cluster to validate their robustness and selectivity using the "best fit" analysis on all training and test set compounds. When a compound is mapped to a hypothesis, the quality of the mapping is expressed by the so-called "fit value". This value is defined as the weight (f) $\times$ [1-SSE(f)], where f is the mapped feature, SSE(f) is the sum over location constraints c on f of $[D(c)/T(c)]$,[2] D is the displacement of

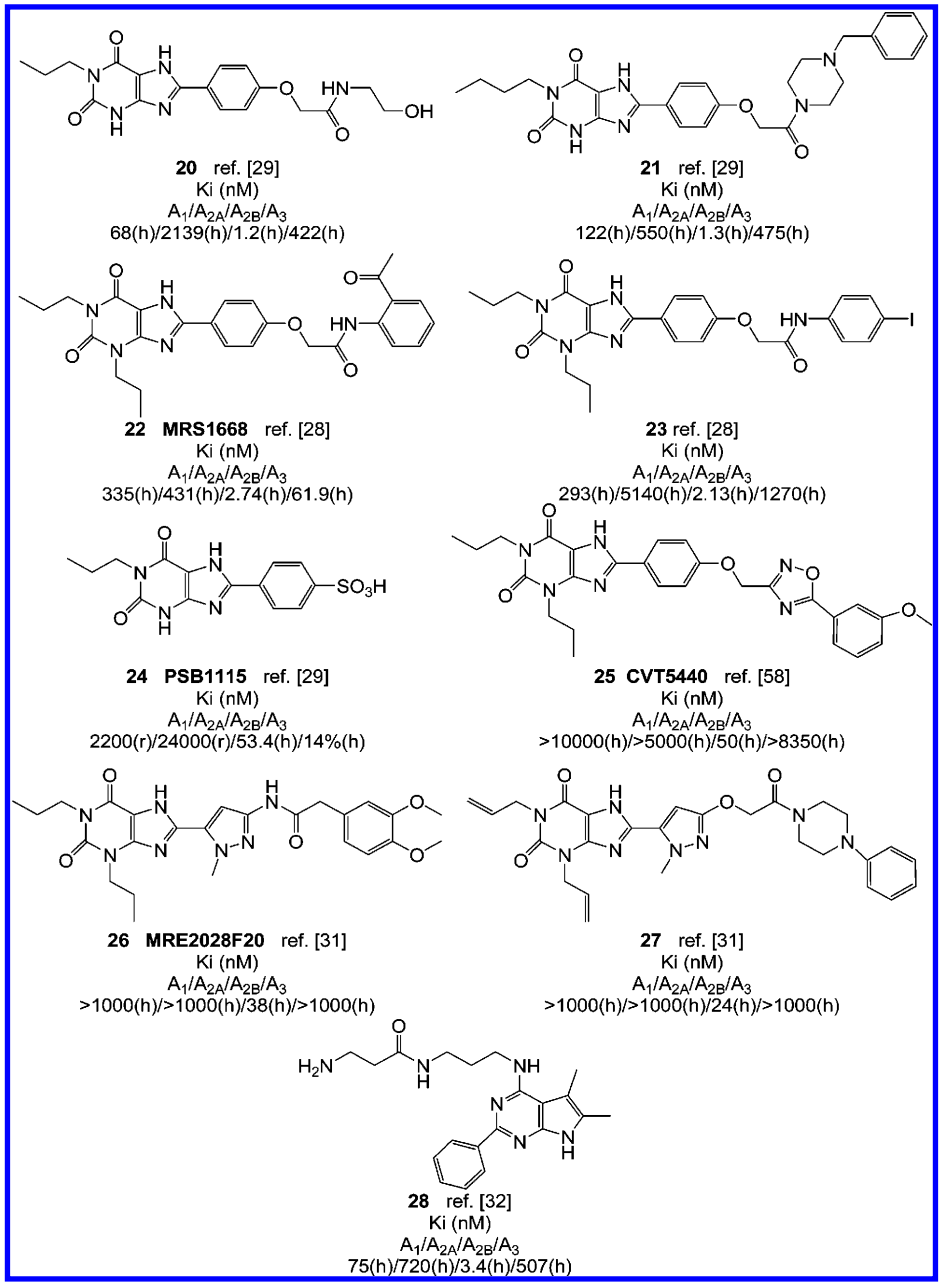

Figure 4. Test set of A_{2B} selective antagonists.

the feature from the center of the location constraint, and *T* (tolerance) is the radius of the location constraint sphere for the feature.[35] Thus, the maximum fit value for a perfectly fitting compound is the sum of the weight values for all features. The minimum value (no fit at all) should be 0. There are two fitting algorithms included in the Catalyst software package: fast fit and best fit. "Fast fit" refers to the method of finding the optimum fit of the substrate to the hypothesis among all the conformers of the molecule without performing an energy minimization on the conformers of the molecule. The "best fit" procedure starts with the fast fit procedure and allows individual conformers to flex over an energy threshold. This allows examination of more conformational space and minimizes the distance between the hypothesis features and the atoms to which they map (Catalyst Tutorials Release 3.0). In this study, we used the best fit analysis to calculate the fit value of every molecule mapped to a pharmacophore model and pick up the hypothesis which gave the highest fit values with both the training set compounds and the corresponding test set molecules.

Third, we built test sets which included antagonists of all AR subtypes with a wide structural diversity to identify the best models that can accurately differentiate A_{2A} and A_{2B} antagonists as well as to evaluate the potential selectivity of the obtained models for A_1 and A_3 antagonists.

Finally, we also evaluated the mapping situation of the best fit conformers of each training and test set molecule on the selected best models to figure out the key features existing in each hypothesis that contributed the most to the selectivities of best models. To this purpose, we evaluated how chemical function groups mapped the corresponding features (i.e., **L**, **R**, **H**, **P**, **Z**) in the pharmacophore models, in addition to the fit values that indicate the total degree of fitness between the compounds and the pharmacophore models. By

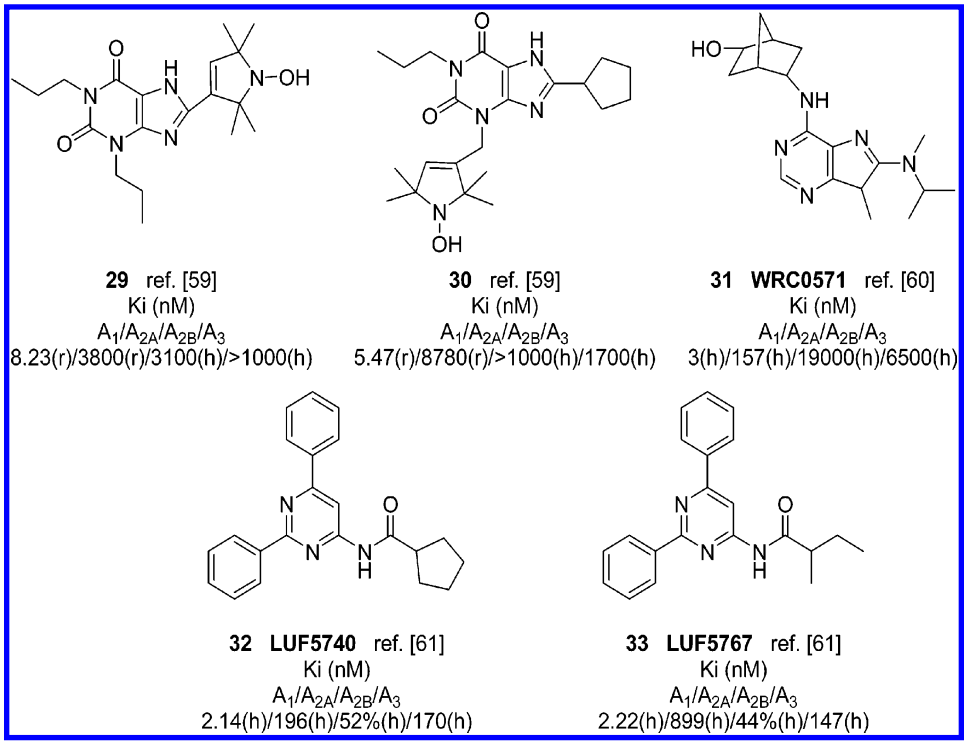

Figure 5. Test set of A_1 selective antagonists.

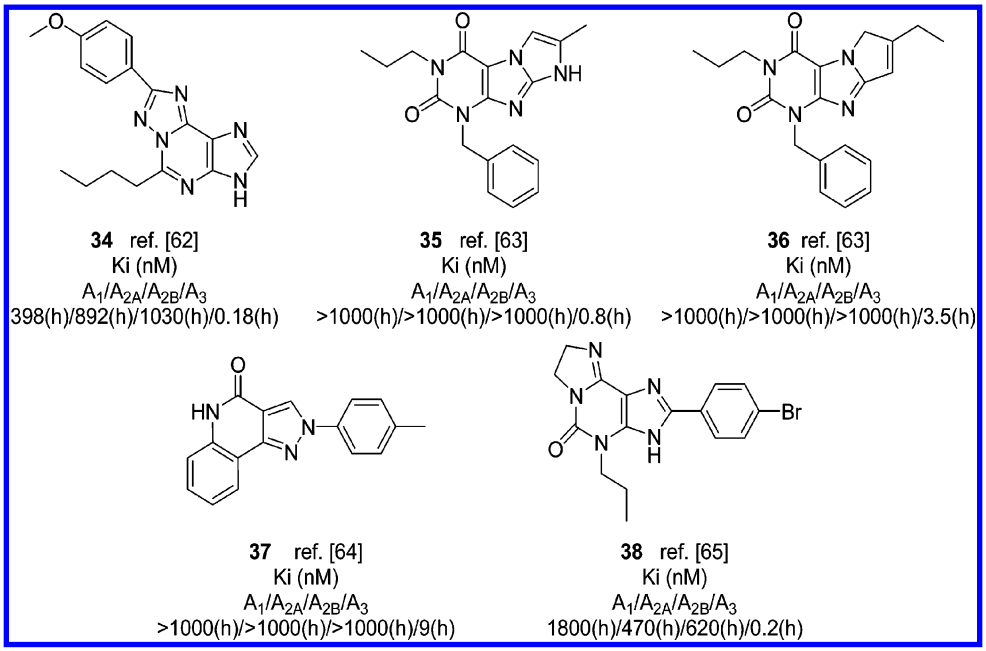

Figure 6. Test set of A_3 selective antagonists.

doing so, we can pick up the most indispensable feature in the hypotheses which play important roles in differentiating selective antagonists for different AR subtypes.

Selection of Test Set Compounds. We collected at least five molecules displaying selective antagonism against each AR subtype to test the robustness and the selectivity of the pharmacophore models previously obtained. Each member of the test set was presented with a collection of conformers that should cover the conformational space of relative energy of 15 kcal/mol above the estimated global energy minimum (following the same conformational search process we used for the training set compounds). After the conformation models were generated, all compounds were forced to map to the pharmacophore models for the best fit analysis and mapping situation check.

In Figures 3−6, we illustrate the structures of the test set compounds for each AR subtype and their binding activities. There were five A_{2A} antagonists (compounds **15**−**19**, Figure 4), which we could not find their binding affinities toward A_{2B} and A_3 from the original literature. However, they had high K_i values for A_{2A} (0.2−14 nM) and showed remarkable selectivity of A_{2A} over A_1 (K_iA_1/K_iA_{2A} from 79 to 16 500). Therefore, we included them for the testing of our A_{2A} pharmacophore models.

Table 3. Summary of Hypotheses for A_{2A} Adenosine Receptor Antagonists

hypothesis[a]	ranking score[b]	composition[c]	cluster[d]
Hypo-A_{2A}-1	68.61	RPL_1L_2	I
Hypo-A_{2A}-4	67.15	RPL_1L_2	
Hypo-A_{2A}-5	67.10	RPL_1L_2	
Hypo-A_{2A}-6	67.00	RPL_1L_2	
Hypo-A_{2A}-7	66.96	RPL_1L_2	
Hypo-A_{2A}-2	67.90	RPLH	II
Hypo-A_{2A}-3	67.90	RPLH	
Hypo-A_{2A}-8	66.81	R_1R_2PL	III
Hypo-A_{2A}-9	66.81	R_1R_2PL	
Hypo-A_{2A}-10	66.79	R_1R_2PL	

[a] Numbers for the hypothesis are consistent with the numeration as obtained by the hypothesis generation. [b] The higher the ranking score, the less likely it is that the molecules in the training set fit the hypothesis by a chance correlation. The best hypotheses have the highest ranks. [c] **R** = ring aromatic group; **P** = positively ionizable group; **L** = hydrogen bond acceptor lipid group; and **H** = hydrophobic group. The same feature type in different models may have different 3D-coordinates. [d] Cluster assembly is adopted from Catalyst's "hypotheses clustering" analysis result based on the composition similarity between hypotheses.

RESULTS AND DISCUSSION

Pharmacophore Model for A_{2A} AR Antagonists. Based on the A_{2A} antagonist training set, ten common features hypotheses were selected according to their ranking scores by the HipHop program (Table 3). Using the hypothesis clustering functionality in Catalyst 4.10, the difference between hypotheses in the feature types and locations as well as the feature composition can be evaluated and categorized. Different numbers of cluster can be obtained from this process, but we decided to focus on the feature similarities and picked up three clusters as presented in Table 3 (all clustering analysis results are described in the Supporting Information).

Cluster I contains five hypotheses with the following features: one ring aromatic feature (**R**), one positively ionizable feature (**P**), and two hydrogen bond acceptor lipid features (**L1** and **L2**). The ranking scores of the hypotheses in this cluster range from 66.96 to 68.61. Cluster II has two hypotheses with the following features: one ring aromatic feature (**R**), one positively ionizable feature (**P**), one hydrophobic feature (**H**), and one hydrogen bond acceptor lipid feature (**L**). Both hypotheses have the same ranking score of 67.90. The three hypotheses for Cluster III all have two ring aromatic features (**R1** and **R2**), one positively ionizable feature (**P**), and one hydrogen bond acceptor lipid feature (**L**), with ranking scores ranging from 66.79 to 66.81.

Only a small difference exists among the ranking scores of the hypotheses in the same cluster, and all cluster members within the same cluster have the same feature types. This suggests that the features of each hypothesis in the same cluster are spatially arranged in a similar way. When checking the 3D alignment for the ten hypotheses, we found they shared three features (**R**, **P**, and **L**). These features show very good overlap in 3D space, indicating they are important for the binding affinity of the A_{2A} antagonists.

One remarkable difference in the feature type among these three clusters was their fourth feature. That is, the hydrogen bond acceptor lipid (**L**) for Cluster I, the hydrophobic region (**H**) for Cluster II, and the ring aromatic feature (**R**) for Cluster III. Except for the hydrogen bond acceptor lipid feature in Cluster I, the latter two features (**H** and **R)** in Clusters II and III displayed the same arrangement and occupied the same location in 3D space because both features were retrieved from the same chemical functional groups of the training set molecules. This seems consistent with the result from Giorgio Tarzia's group, in which their computational modeling for the A_{2A} receptor also indicated a hydrophobic interaction or a ring aromatic region at this position.[48]

The 2D representations of hypotheses and distances between features for the top-scored model of each cluster are shown in Figure 7.

Best Model Selection for A_{2A} AR Antagonists. Following the aforementioned basic strategy, we performed a three-step validation process to find the best model from the generated A_{2A} hypotheses. The process was as follows: (1) Take the three top-scored hypotheses and run the retrieve analysis toward the training set molecules. (2) Run the best fit analysis using test set A_{2A} antagonists in order to validate the predictiveness of each hypothesis. (3) Carry out best fit analysis on the other three external test sets of A_{2B}, A_1, and A_3 antagonists to further evaluate the potential selectivity of the pharmacophore models. In our case, the statistically best hypothesis model obtained from such a validation process was the Hypo-A_{2A}-2 from Cluster II, which has the feature combination of **RPHL**. We renamed this best model as Hypo-A_{2A}. Table 4 lists the mapping analysis results and the best fit values for the A_{2A} antagonist training set and the three external test sets, which consist of 9 A_{2A} AR antagonists (compounds **11**−**19**), 14 A_{2B} AR antagonists (compounds **6**−**10** and **20**−**28**), 5 A_1 antagonists (compounds **29**−**33**), and 5 A_3 antagonists (compounds **34**−**38**).

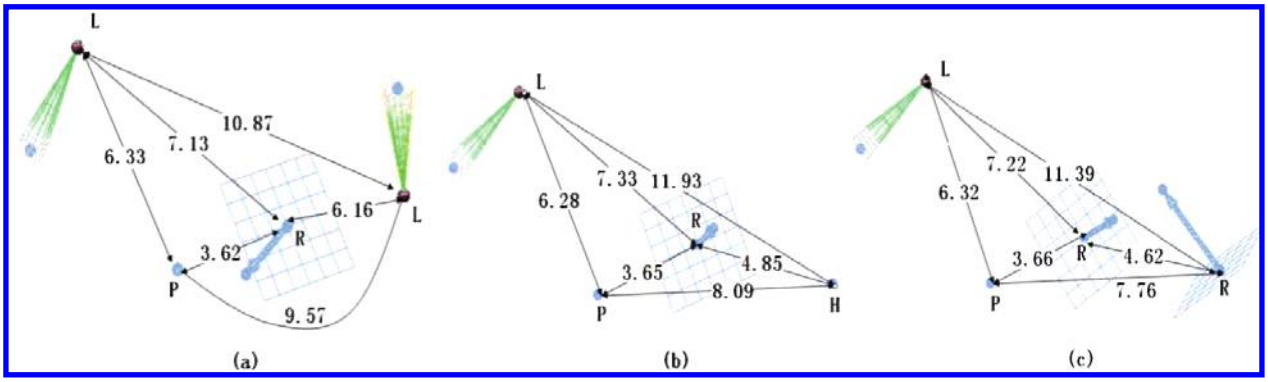

Figure 7. Three representative hypothesis models for A_{2A} selective antagonists: (a) Hypo-A_{2A}-1 of cluster I; (b) Hypo-A_{2A}-2 of cluster II; and (c) Hypo-A_{2A}-8 of cluster III; **R** = ring aromatic; **H** = hydrophobic; **L** = hydrogen bond acceptor lipid; and **P** = positively ionizable.

Table 4. Best Fit Values (Fit) of the A_{2A} Training Set and All Test Sets Mapped on the Best Model Hypo-A_{2A}[50]

A_{2A} training set						A_{2A} test set					
		mapped feature[c]						mapped feature[c]			
no.[a]	fit[b]	R	P	L	H	no.[a]	fit[b]	R	P	L	H
1	3.99	+	+	+	+	**11**	3.79	+	+	+	+
2	4.00	+	+	+	+	**12**	2.99	+	+	+	−
3	3.19	+	+	+	+	**13**	3.99	+	+	+	+
4	3.99	+	+	+	+	**14**	3.69	+	+	+	+
5	3.99	+	+	+	+	**15**	3.70	+	+	+	+
						16	3.70	+	+	+	+
						17	3.67	+	+	+	+
						18	3.42	+	+	+	+
						19	3.53	+	+	+	+

A_{2B} test set						A_1 and A_3 test sets					
		mapped feature[c]						mapped feature[c]			
no.[a]	fit[b]	R	P	L	H	no.[a]	fit[b]	R	P	L	H
6	2.75	+	−	+	+			A_1			
7	2.85	+	−	+	+	**29**	1.86	+	−	+	−
8	2.04	−	−	+	+	**30**	1.94	+	−	+	−
9	2.00	−	−	+	+	**31**	2.76	+	+	+	−
10	2.10	+	−	+	+	**32**	1.99	+	−	−	+
20	1.96	−	+	+	−	**33**	1.99	+	−	−	+
21	2.97	+	−	+	+						
22	2.00	−	−	+	+			A_3			
23	2.04	−	−	+	+	**34**	1.96	+	−	−	−
24	2.71	+	−	+	+	**35**	2.00	+	+	−	−
25	2.74	+	−	+	+	**36**	1.96	+	−	−	+
26	2.30	+	−	+	+	**37**	1.98	+	−	−	+
27	2.00	−	−	+	+	**38**	1.96	+	−	−	+
28	2.97	+	−	+	+						

[a] Compound numbers and chemical structures are depicted in Figures 1−6. [b] The number represents the best fit of each molecule to the hypothesis. The higher the best fit value is, the better a molecule maps the features of a hypothesis. The best fit value of 4.00 means a perfect mapping of the molecule to the hypothesis. [c] The "+" sign means the chemical feature of a compound maps the corresponding feature of the hypothesis. The "−" sign means the compound misses the mapping of the corresponding hypothesis feature, or the compound does not have such a chemical feature to map the corresponding feature of the hypothesis.

The best fit value and mapping results in Table 4 demonstrate that the selected A_{2A} AR antagonists map the **R**, **P**, **H**, and **L** features of the best model Hypo-A_{2A}, except for compound **12,** which does not simultaneously map the **H** feature due to its rigid structure and small molecular size. A_{2B} receptor antagonists map only the **R**, **H**, and **L** features of the best model Hypo-A_{2A}, while none maps the positively ionizable region (**P**). Further, none of the A_1 and A_3 AR antagonists can fit the Hypo-A_{2A} very well—even after setting the "max omitted feature" value to 1 which allows the compounds to miss one hypothesis feature, except for compound **31,** which maps three of the Hypo-A_{2A} features, possibly due to the flexibility of its structure and high A_{2A} AR binding affinity (K_i=157 nM). However, its best fit value is only 2.76.

The SAR study of tricyclic A_{2A} derivatives by Baraldi's[21] group indicated that some structural characteristics (i.e., tricyclic structure, free amino group at 5-position, and furan ring) are important for the binding affinity of the A_{2A} antagonists. Our best fit analysis of tricyclic compounds against Hypo-A_{2A} indicated that the ring aromatic region is occupied by the pyrazolo ring of the tricyclic structure, the positively ionizable region is occupied by the amino group at 5-position, the hydrogen bond acceptor lipid region is occupied by the oxygen on the furan ring, and the hydrophobic region is occupied by the phenyl ring on the side chain at 7-position. Figure 8 shows the mapping alignment of the chemical functional groups of triazolo pyrimidine A_{2A} antagonists in the training set with the best model Hypo-A_{2A}.

Figure 8. Best model Hypo-A_{2A} mapped with selective A_{2A} antagonists in the training set (compound **1**: yellow, **2**: green, **3**: blue, **4**: red, **5**: cyan). Pharmacophore features are color-coded: green represents hydrogen bond acceptor lipid (**L**); orange represents ring aromatic (**R**); light blue represents hydrophobic (**H**); and red represents positively ionizable (**P**). Compound numbers and chemical structures are depicted in Figure 1.

The best fit analysis results of model Hypo-A_{2A} (summarized in Table 4) suggest that the ring aromatic, positively ionizable, hydrophobic, and hydrogen bond acceptor lipid groups are important for activity in the A_{2A} AR antagonists and that the positively ionizable group may be related to the selectivity for A_{2A} AR over A_{2B} and other AR subtypes.

In Figure 9(a),(b), we illustrated with two mapping examples to explain the difference of the mapping situation of Hypo-A_{2A} mapped with A_{2A} test set compounds versus A_{2B} test set compounds (more mapping analysis results are described in the Supporting Information). Figure 9(a) displays that the A_{2A} test set compounds are mapped well with all features in Hypo-A_{2A} with high best fit values: compound **15**, 3.70; compound **16**, 3.70; and compound **19**, 3.53. In contrast, Figure 9(b) shows that the A_{2B} test set compounds **6**−**8** are missing at least one hypothesis feature when mapped with Hypo-A_{2A}. Therefore, the best fit values for these three compounds are as follows: compounds **6**, 2.75; **7**, 2.85; and **8**, 2.04.

Pharmacophore Model for A_{2B} AR Antagonists. Following the same clustering analysis process we performed on A_{2A} antagonists, we again chose three clusters of hypotheses for the A_{2B} selective antagonists training set (more details are described in the Supporting Information). All three clusters contain the same four feature types: one ring aromatic feature (**R**), one hydrophobic aliphatic feature (**Z**), and two hydrogen bond acceptor lipid features (**L1** and **L2**). The difference between each cluster lies in the 3D arrangement of hypothesis features (3D location), which HipHop picks up from different conformer alignments or different functional groups in the training set molecules. Among these four features, the ring aromatic (**R**) and the hydrophobic aliphatic (**Z**) consistently maintain their location in each model and map the corresponding functional groups in all molecules for the training set. However, the two hydrogen bond acceptor lipid features (**L1** and **L2**) vary their positions slightly from cluster to cluster (Table 5).

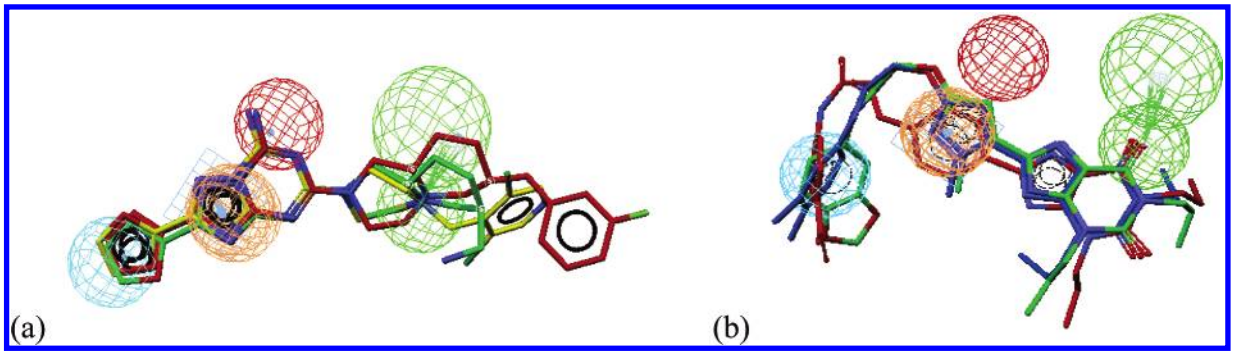

Figure 9. (a) Best model Hypo-A_{2A} mapped with selective A_{2A} antagonists nos. **15** (red), **16** (green), and **19** (yellow) in the A_{2A} test set. All hypothesis features are mapping with the corresponding chemical functional groups on the antagonists. (b) Best model Hypo-A_{2A} mapped with selective A_{2B} antagonists nos. **6** (red), **7** (green), and **8** (blue) in the A_{2B} test set. All ligands miss at least one hypothesis feature (e.g., the positively ionizable sphere). Pharmacophore features are color-coded: green represents hydrogen bond acceptor lipid (**L**); orange represents ring aromatic (**R**); light blue represents hydrophobic (**H**); and red represents positively ionizable (**P**). Compound numbers and chemical structures are depicted in Figures 2 and 3.

Table 5. Summary of Hypotheses for A_{2B} Adenosine Receptor Antagonists

hypothesis[a]	ranking score[b]	composition[c]	cluster[d]
Hypo-A_{2B}-1	85.43	RZL_1L_2	I
Hypo-A_{2B}-2	85.43	RZL_1L_2	
Hypo-A_{2B}-3	82.58	RZL_1L_2	
Hypo-A_{2B}-6	81.56	RZL_1L_2	
Hypo-A_{2B}-9	80.44	RZL_1L_2	
Hypo-A_{2B}-4	81.73	RZL_1L_2	II
Hypo-A_{2B}-5	81.69	RZL_1L_2	
Hypo-A_{2B}-7	81.29	RZL_1L_2	
Hypo-A_{2B}-10	80.40	RZL_1L_2	
Hypo-A_{2B}-8	80.44	RZL_1L_2	III

[a] Numbers for the hypothesis are consistent with the numeration as obtained by the hypothesis generation. [b] The higher the ranking score is, the less likely it is that the molecules in the training set fit the hypothesis by a chance correlation. The best hypotheses have the highest ranking scores. [c] **R** = ring aromatic group; **Z** = hydrophobic aliphatic; and **L** = hydrogen bond acceptor lipid group. The same feature type in different models may have different 3D-coordinates. [d] Cluster assembly is adopted from Catalyst's "hypotheses clustering" analysis result based on the composition similarity between hypotheses.

Table 6. Fit Values (Fit) and Mapped Features of the A_{2B} Training Set Molecule to the Hypotheses

	Hypo-A_{2B}-1		Hypo-A_{2B}-4		Hypo-A_{2B}-8	
no.[a]	fit[b]	mapped feat.[c]	fit[b]	mapped feat.[c]	fit[b]	mapped feat.[c]
6	2.99	RZL_1	3.00	RZL_1	4.00	RZL_1L_2
7	4.00	RZL_1L_2	3.50	RZL_1L_2	2.99	RL_1L_2
8	2.82	RZL_1	2.83	RZL_1	3.35	RZL_1L_2
9	3.90	RZL_1L_2	3.00	RZL_1	3.00	RL_1L_2
10	3.75	RZL_1L_2	3.81	RZL_1L_2	2.98	RL_1L_2

[a] Compound numbers and chemical structures are depicted in Figures 1−6. [b] The number represents the best fit of each molecule to the hypothesis. The higher the best fit value is, the better a molecule maps the features of a hypothesis. The best fit value of 4.00 means a perfect mapping of the molecule to the hypothesis. [c] **R** = ring aromatic group; **Z** = hydrophobic aliphatic; and **L** = hydrogen bond acceptor lipid group. The same feature type in different model may have different 3D-coordinates.

Table 6 summarizes the best fit analysis results of the training set molecules using the three top-scored pharmacophore models from each cluster. The results indicate the program performed very well on recognizing at least three common features for all training set molecules. However, unlike the A_{2A} hypotheses, each of the selected A_{2B} models misses one feature for some of the training set molecules (best fit value ranged from 3.00 to 4.00). The reason for the missing features is perhaps due to the flexibility and assorted feature distribution of the training set molecules.

In case the Catalyst generates hypotheses which may not have been sufficient to mimic all of the training set compounds, it is often productive to merge or modify certain hypotheses to obtain a new hypothesis with a more satisfying result.[49]

In order to create a comprehensive hypothesis model based on the obtained HipHop models, we initially tried to use the program's "merge tool" to combine two models. Our attempts to merge two hypotheses from different clusters only produced the new five-featured models due to the nonmergeable distance between two of the hydrogen bond acceptor lipid features in different hypotheses. Unfortunately, these five-featured new hypotheses were unable to yield the desired results in terms of the best fit value and feature mapping analysis.

Therefore, the best model containing all important features and fulfilling the selection criteria for the best hypothesis was finally created using a manual modification technique from the top-scored hypotheses in Cluster I and Cluster II (Hypo-A_{2B}-1 and Hypo-A_{2B}-4). The procedure entailed the following:

(1) Running "best fit compare" using the most active A_{2B} antagonist **7** with Hypo-A_{2B}-1 (Figure 10(a)) and then reserving this "active configuration" of compound **7** as a template because it mapped Hypo-A_{2B}-1 satisfactorily, with a perfect fit value of 4.00. This template had the following four features: two hydrogen bond acceptor lipid (**L1** and **L2**); one ring aromatic (**R**); and one hydrophobic aliphatic (**Z**).

(2) Creating another hydrogen bond acceptor lipid feature on the ethereal oxygen in the middle of the above template molecule by using the "Chemical Feature-Based Hypothesis Generation" tool in Catalyst. The reason for making this new feature on the ethereal oxygen was based on the result of the mapping analysis of the training set compounds to Hypo-A_{2B}-4, where all molecules had satisfactorily mapped their ethereal oxygen atoms with a hydrogen bond acceptor lipid sphere (Figure 10(b)).

(3) Erasing the hydrogen bond acceptor lipid feature on the terminal of the molecule.

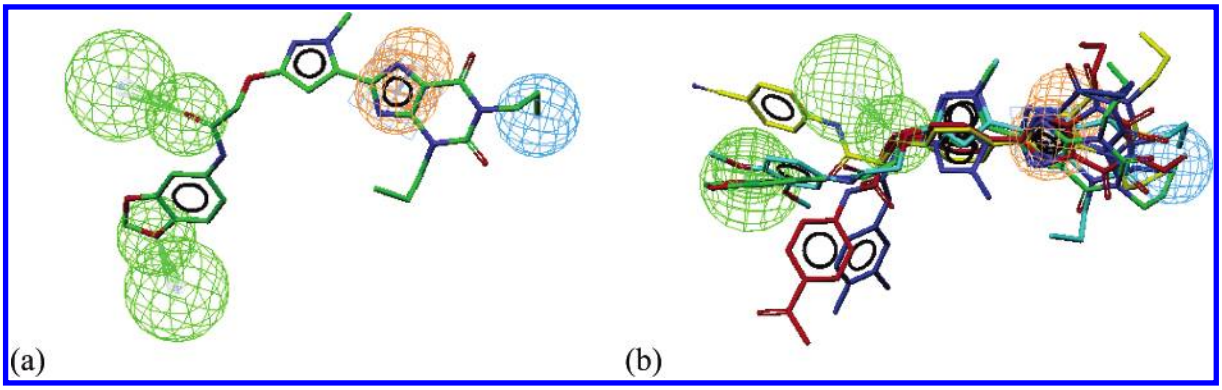

Figure 10. (a) Template conformer of compound **7** mapped with Hypo-A_{2B}-1. (b) Commonly shared features in Hypo-A_{2B}-4: the hydrogen bond acceptor lipid feature mapped the ethereal oxygen by all training set molecules (compounds **6** (red), **7** (green), **8** (blue), **9** (yellow), and **10** (cyan)). Pharmacophore features are color-coded: green represents hydrogen bond acceptor lipid (**L**); orange represents ring aromatic (**R**); and light blue represents hydrophobic aliphatic (**Z**). The chemical structure of compound **7** is depicted in Figure 2.

Table 7. Best Fit Values (Fit) of the A_{2B} Training Set and All Test Sets Mapped on the Best Model Hypo-A_{2B}[50]

A_{2B} training set						A_{2B} test set					
		mapped feature[c]						mapped feature[c]			
no.[a]	fit[b]	R	Z	La	Lb	no.[a]	fit[b]	R	Z	La	Lb
6	3.81	+	+	+	+	**20**	3.80	+	+	+	+
7	4.00	+	+	+	+	**21**	3.66	+	+	+	+
8	3.97	+	+	+	+	**22**	3.88	+	+	+	+
9	3.84	+	+	+	+	**23**	3.91	+	+	+	+
10	3.99	+	+	+	+	**24**	3.20	+	+	+	+
						25	3.88	+	+	+	+
						26	3.49	+	+	+	+
						27	3.89	+	+	+	+
						28	3.77	+	+	+	+

A_{2A} test set						A_1 and A_3 test sets					
		mapped feature[c]						mapped feature[c]			
no.[a]	fit[b]	R	Z	La	Lb	no.[a]	fit[b]	R	Z	La	Lb
1	2.00	+	+	−	−			A_1			
2	2.80	+	+	−	+	**29**	2.92	+	+	+	−
3	2.65	+	+	−	+	**30**	2.00	+	+	−	−
4	2.00	+	+	−	−	**31**	2.00	+	−	+	−
5	2.00	+	+	−	−	**32**	1.99	+	+	−	−
11	2.13	−	+	+	+	**33**	2.40	+	−	+	+
12	1.00	+	+	−	−						
13	2.00	+	+	−	−			A_3			
14	2.78	−	+	+	+	**34**	2.77	+	+	+	−
15	2.00	+	+	−	−	**35**	2.00	+	+	−	−
16	1.99	+	+	−	−	**36**	2.28	+	+	+	−
17	2.00	+	+	−	−	**37**	1.78	+	−	+	−
18	1.99	+	+	−	−	**38**	1.98	+	+	−	−
19	1.97	+	+	−	−						

[a] Compound numbers and chemical structures are depicted in Figures 1−6. [b] The number represents the best fit of each molecule to the hypothesis. The higher the best fit value is, the better a molecule maps the features of a hypothesis. The best fit value of 4.00 means a perfect mapping of the molecule to the hypothesis. [c] The "+" sign means the chemical feature of a compound maps the corresponding feature of the hypothesis. The "−" sign means the compound misses the mapping of the corresponding hypothesis feature, or the compound does not have such a chemical feature to map the corresponding feature of the hypothesis.

(4) Merging the newly created hydrogen bond acceptor lipid feature with the other three original features in the template model to form a new four-featured hypothesis. We kept the hydrogen bond acceptor lipid feature on the carbonyl oxygen from the Hypo-A_{2B}-1 hypothesis because this feature is commonly occupied by all the training set molecules in mapping analysis.

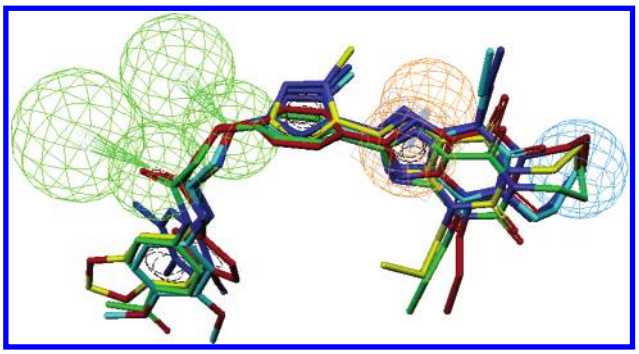

Figure 11. Manually generated A_{2B} antagonist hypothesis Hypo-A_{2B} mapped with selective A_{2B} antagonists in the training set. Pharmacophore features are color-coded: green represents hydrogen bond acceptor lipid (**L**); orange represents ring aromatic (**R**); and light blue represents hydrophobic aliphatic (**Z**). Compound numbers and chemical structures as depicted in Figure 2 (compounds **6**, green; **7**, yellow; **8**, blue; **9**, red; and **10**, cyan).

The manually generated new hypothesis from Hypo-A_{2B}-1 and Hypo-A_{2B}-4 contains four features: one hydrophobic aliphatic feature (**Z**), one ring aromatic feature (**R**), one hydrogen bond acceptor lipid feature (**La**) manually created from the ethereal oxygen, and another hydrogen bond acceptor lipid feature (**Lb**) taken from Hypo-A_{2B}-1, which mapped to the carbonyl oxygen. This hypothesis was then tested against all training set molecules to show satisfactory feature mapping and best fit value (Table 7). We named this manually generated best model for A_{2B} antagonist Hypo-A_{2B}. The mapping alignment of all training set compounds to Hypo-A_{2B} is shown in Figure 11.

Validation and Selectivity Evaluation of the Best Model for A_{2B} AR Antagonists. Table 7 summarizes the best fit analysis results using the aforementioned best model Hypo-A_{2B} for selecting the A_{2B} antagonists in the test set as well as the A_1 and A_3 selective antagonists test compounds. High best fit values were recorded for all the A_{2B} selective antagonists (3.20−4.00), whereas most of the A_{2A} selective antagonists were unable to map one or both of the hydrogen bond acceptor lipid features using this A_{2B} hypothesis model. This suggests that these hydrogen bond acceptor regions play an important role in A_{2A}/A_{2B} selectivity. In addition, the mapping results in Table 7 (see results: A1 and A3 test set) indicate that the hydrogen bond acceptor feature on the terminal of the best model (**Lb**) might be the key area for the differentiation of A_{2B} from A_1 and A_3 antagonists.

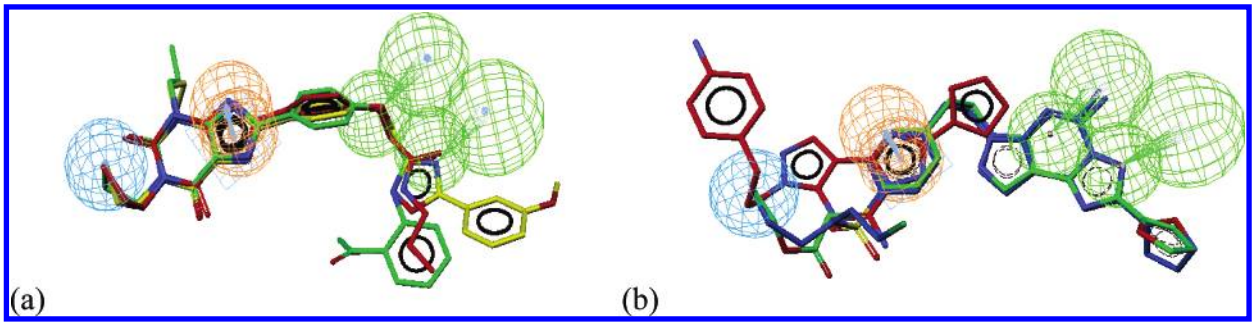

Figure 12. (a) Best model Hypo-A_{2B} mapped with selective A_{2B} antagonists nos. **20** (red), **22** (green), and **25** (yellow) in the A_{2B} test set. All hypothesis features are mapped with the corresponding chemical functional groups on the antagonists. (b) Best model Hypo-A_{2B} mapped with selective A_{2A} antagonists nos. **1** (red), **2** (green), and **3** (blue) in the A_{2A} test set. All ligands miss at least one hypothesis feature of the hydrogen bond acceptor lipid. Pharmacophore features are color-coded: green represents hydrogen bond acceptor lipid (**La** and **Lb**); orange represents ring aromatic (**R**); and light blue represents hydrophobic aliphatic (**Z**). Compound numbers and chemical structures are depicted in Figures 1 and 4.

According to the mapping analysis result in Table 7, Figure 12(a),(b) show some examples on the mapping differences between the Hypo-A2B/A_{2B} test set and the Hypo-A2B/A_{2A} test set (more mapping results are described in the Supporting Information).

For the purpose of illustration, three selected A_{2B} test set molecules (compounds **20, 22**, and **25**) are mapped to Hypo-A_{2B} where all pharmacophore features are well occupied by the corresponding chemical functional groups of the compounds (Figure 12(a)). This is consistent with the high best fit values obtained from the mapping analysis of these molecules. It can be seen from Figure 12(b) that compound **1** (red) has missed both the hydrogen bond acceptor lipid features and both compounds **2** (green) and **3** (blue) have missed one of the hydrogen bond acceptor lipid features in Hypo-A_{2B}.

Zefirov's group has recently used computational molecular modeling to propose a model for the human A_{2B} adenosine receptor.[2] All four features of our hypothesis model Hypo-A_{2B} correspond well to each of the residue areas in their receptor model: the hydrophobic region (**H**) corresponds to the lipophilic pocket formed by Leu49, Asp53, Asn286, and Pro287; the ring aromatic region (**R**) corresponds to the interaction area involving Trp247; the hydrogen bond acceptor region on the ethereal oxygen (**La**) corresponds to the residue Thr89; and the hydrogen bond acceptor feature on carbonyl oxygen (**Lb**) corresponds to the hydrogen bond donor Asn186.

To further confirm the selectivity of our A_{2B} model, we tested this hypothesis against two highly selective xanthine type A_{2A} antagonists, BS-DMPX (7-methyl-8-(3-bromostyryl)-3,7-dimethyl-1-propargylxanthine) and MSX-2 (3-(3-hydroxypropyl)-7-methyl-8-(3-methoxystyryl)-1-propargylxanthine), which are well-known from a series of studies.[51] Their best fit values were 2.0 and 2.99, respectively, and the corresponding best fit conformer energies were 8.24 kcal/mol for BS-DMPX and 10.38 kcal/mol for MSX-2. The poor mapping result was caused by a lack of potential hydrogen bond mediators, such as heteroatoms, in their side-chain structures at the 8-position (Figure 13).

Comparison between the Best Models for A_{2A} and A_{2B}. From the best fit validation and the mapping analysis, we identified that both A_{2A} and A_{2B} antagonist pharmacophore models (Hypo-A_{2A} and Hypo-A_{2B}) consist of essential features necessary for compounds to be highly active and selective toward their corresponding receptor subtype. In Figure 14, we superimposed the common features of Hypo-A_{2A} and Hypo-A_{2B} using the "hypothesis compare" process. The positively ionizable feature (**P**) is commonly shared by A_{2A} antagonists, but it cannot be mapped by A_{2B} and most A_1 and A_3 selective antagonists, indicating that this feature is one of the key areas for A_{2A} selectivity (see Table 4). In the Hypo-A_{2A} pharmacophore model, all four features—the ring aromatic feature (**R**), the positively ionizable region (**P**) together with the hydrogen bond acceptor lipid (**L**), and the hydrophobic feature (**H**) (the highlighted features in Figure 14)—are important common features for the binding of all A_{2A} antagonists. Compounds mapping all features together are considered potential A_{2A} selective antagonists.

In the hypothesis model Hypo-A_{2B}, the four features (hydrophobic alphatic (**Z**), ring aromatic (**R**) and two hydrogen bond acceptor lipid (**La** and **Lb**)) are essential for all A_{2B} selective antagonists, as they were occupied by all training- and test-set A_{2B} compounds. The key feature that differentiates A_{2B} antagonists from A_{2A} selective compounds most likely comes from one or both of the hydrogen bond acceptor lipid functions in the A_{2B} model, since A_{2A} selective compounds miss at least one of these A_{2B} features, especially in the hydrogen bond acceptor lipid area.

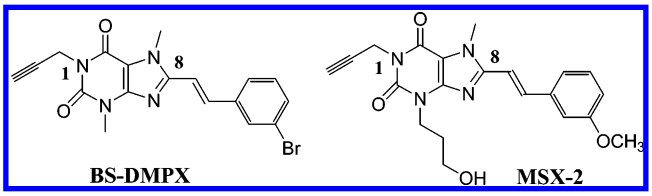

Figure 13. Selective xanthine type A_{2A} antagonists.

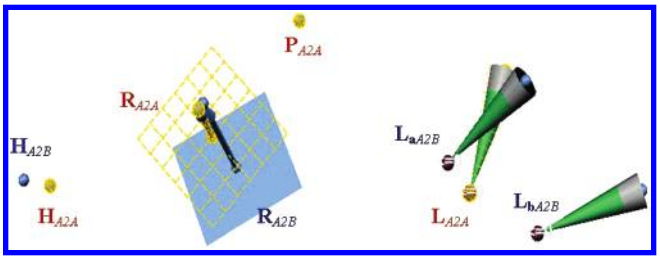

Figure 14. The comparison of Hypo-A_{2A} with Hypo-A_{2B}. Pharmacophore features: **R** = ring aromatic; **H** = hydrophobic; **Z** = hydrophobic aliphatic; **L** = hydrogen bond acceptor lipid; and **P** = positively ionizable. HypoA_{2A} is highlighted with yellow spheres. Distances between the same feature types: $D_{HA2A-HA2B} = 1.21$ Å; $D_{RA2A-RA2B} = 1.13$ Å; and $D_{LA2A-LaA2B} = 1.10$ Å.

CONCLUSION

Both pharmacophore models generated for A_{2A} and A_{2B} antagonists in this study highlight the structural requirements for antagonistic activity and selectivity on adenosine receptor antagonists. In this work, two different processes were performed to develop the essential pharmacophore for A_{2A} and A_{2B} antagonists. The best pharmacophore model Hypo-A_{2A} for A_{2A} AR antagonists was obtained through the validation process from the top-scored hypotheses of three clusters. Hypo-A_{2A} consisted of four features: one ring aromatic feature, one positively ionizable feature, one hydrophobic feature, and one hydrogen bond acceptor lipid feature. The best pharmacophore model for A_{2B} antagonists was manually created based on two HipHop models generated from the selective A_{2B} antagonist training set. It is characterized by the following four features: one ring aromatic feature, one hydrophobic aliphatic feature, and two hydrogen bond acceptor lipid features. Both pharmacophore models can identify the corresponding A_{2A} and A_{2B} antagonists as direct hits in the training sets. Moreover, both the best Hypo-A_{2A} and Hypo-A_{2B} models could perfectly differentiate all other subtype antagonists in the test sets. All features in each model are essential for both receptor binding activity and selectivity. Compounds that can map all features in the pharmacophore model will be considered as potent and selective A_{2A} and A_{2B} antagonists.

The purpose of pharmacophore models is to perform in silico screening searches in a 3D database of a virtual or real compound library to find diverse structures with desired binding activity and selectivity. We plan to use the models we generated to design and discover novel selective A_{2A} and A_{2B} AR antagonists, especially the non-xanthine type antagonists, as pharmaceutical candidates.

EXPERIMENTAL SECTION

All of this study was performed using Catalyst 4.10 installed on a IBM6223I2C work station equipped with an Intel Xeon processor (3.0 GHz) and 1GB of RAM running the RedHat WS3.0 operating system.

ACKNOWLEDGMENT

We thank Ms. Songmei Li, Ms. Wei Wang, and Dr. Zhanli Wang at NEOTRIDENT as well as Dr. Brian Sung at Accelrys, Inc., for their dedicated support.

Supporting Information Available: Log files and clustering analysis results for HipHop hypotheses from A_{2A} and A_{2B} antagonists and best fit analysis results of Hypo-A_{2A} andn Hypo-A_{2B} toward their training set and test set compounds. This material is available free of charge via the Internet at http://pubs.acs.org.

REFERENCES AND NOTES

(1) Fredholm, B. B.; IJzerman, A. P.; Jacobson, K. A.; Klotz, K. N.; Linden, J. International union of pharmacology. XXV. nomenclature and classification of adenosine receptors. *Pharmacol. Rev.* **2001**, *53*, 527−552.

(2) Ivanov, A. A.; Baskin, I. I.; Palyulin, V. A.; Piccagli, L.; Baraldi, P. G.; Zefirov, N. S. Molecular modeling and molecular dynamics simulation of the human A2B adenosine receptor. The study of the possible binding modes of the A2B receptor antagonists. *J. Med. Chem.* **2005**, *48*, 6813−6820.

(3) Hourani, S. M.; Boon, K.; Fooks, H. M.; Prentice, D. J. Role of cyclic nucleotides in vasodilations of the rat thoracic aorta induced by adenosine analogues. *Br. J. Pharmacol.* **2001**, *133*, 833−840.

(4) Richardson, P. J.; Kase, H.; Jenner, P. G. Adenosine A2A receptor antagonists as new agents for the treatment of Parkinson's disease. *Trends Pharmacol. Sci.* **1997**, *18*, 338−344.

(5) Ongini, E.; Adami, M.; Ferri, C.; Bertorelli, R. Adenosine A2A receptors and neuroprotection. *Ann. N. Y. Acad. Sci.* **1997**, *825*, 30−48.

(6) Elenkov, I. J.; Chrousos, G. P.; Wilder, R. L. Neuroendocrine regulation of IL-2 and TNF-alpha/IL-10 balance, clinical implications. *Ann. N. Y. Acad. Sci.* **2000**, *917*, 94−105.

(7) Varani, K.; Rigamonti, D.; Sipione, S.; Camurri, A.; Borea, P. A.; Cattabeni, F.; Abbracchio, M. P.; Cattaneo, Elena. Aberrant amplification of A2A receptor signaling in striatal cells expressing mutant huntingtin. *FASEB* **2001**, *15*, 1245−1247.

(8) Ryzhov, S.; Goldstein, A. E.; Matafonov, A.; Zeng, D.; Biaggioni, I.; and Feoktistov, I. Adenosine-activated mast cells induce IgE synthesis by B lymphocytes: An A_{2B}-mediated process involving Th2 cytokines IL-4 and IL-13 with implications for asthma. *J. Immunol.* **2004**, *172*, 7726−7733.

(9) Jr, J. H.; Obikao, B.; Thompson, W. J.; Downey, J. Adenosine induced vasodilation: receptor characterization in pulmonary circulation. *Am. J. Physiol.* **1995**, *268*, 1862−1868.

(10) Dubey, R. K.; Gillespie, D. G.; Mi, Z.; Jackson, E. K. Adenosine inhibits growth of human aortic smooth muscle cells via A2B receptors. *Hypertension* **1998**, *31*, 516−521.

(11) Murthy, K. S.; McHenry, L.; Grider, J. R.; Makhlouf, G. M. Adenosine A_1 and A_{2B} receptors coupled to distinct interactive signaling pathways in intestinal muscle cells. *J. Pharmacol. Exp. Ther.* **1995**, *274*, 300−306.

(12) Neary, J. T.; Rathbone, M. P.; Cattabeni, F.; Abbracchio, M. P.; Burnstock, G. Trophic actions of extracellular nucleotides and nucleosides on glial and neuronal cells. *Trends Neurosci.* **1996**, *19*, 13−18.

(13) Feokistov, I.; Biaggioni, I. Pharmalogical characterization of adenosine A2B receptors. *Biochem. Pharmacol.* **1998**, *55*, 627−633.

(14) Vassallo, R.; Lipsky, J. J. Theophylline: recent advances in the understanding of its mode of action and uses in clinical practice. *Mayo Clin. Proc.* **1998**, *73*, 346−354.

(15) Drazen, J. M.; Israel, E.; O'Byrne, P. M. Treatment of asthma with drugs modifying the leukotriene pathway. *N. Engl. J. Med.* **1999**, *340*, 197−206.

(16) Howell, R. E.; Muehsam, W. T.; Kinnier, W. J. Mechanism for the emetic side effect of xanthine bronchodilators. *Life Sci.* **1990**, *46*, 563−568.

(17) (a) IJzerman, A. P.; van der Wenden, E. M.; van Galen, P. J.; Jacobson, K. A. Molecular modeling of adenosine receptors. The ligand binding site on the rat adenosine A2A receptor. *Eur. J. Pharmacol.* **1994**, Jun 15; *268* (1), 95−104. (b) Doytchinova, I.; Valkova, I.; Natcheva, R. CoMFA Study on Adenosine A2A Agonists. *Quantitative Structure-Activity Relationships* **2001**, *20*, 124−129. (c) Song, Y.; Coupar, I. M.; Iskander, M. N. *Quant. Struct.−Act. Relat.* **2001**, *20*, 23−30.

(18) Nonaka, Y.; Shimada, J.; Nonaka, H.; Koike, N.; Aoki, N.; Kobayashi, H.; Kase, H.; Yamaguchi, K.; Suzuki, F. Photoisomerization of a potent and selective adenosine A2 antagonist, (E)-1,3-dipropyl-8-(3,4-dimethoxystyryl)-7-methylxanthine. *J. Med. Chem.* **1993**, *36*, 3731−3733.

(19) (a) Müller, C. E.; Sandoval-Ramírez, J.; Schobert, U.; Geis, U.; Frobenius, W.; Klotz, K. N. 8-(Sulfostyryl)xanthines: water-soluble A2A-selective adenosine receptor antagonists. *Bioorg. Med. Chem.* **1998**, *6*, 707−719. (b) Müller, C. E.; Geis, U.; Hipp, J.; Schobert, U.; Frobenius, W.; Pawlowski, M.; Suzuki, F.; Sandoval-Ramírez, J. Synthesis and structure-activity relationship of 3,7-dimethyl-1-propargylxanthine derivatives, A2A-selective adenosine receptor antagonists. *J. Med. Chem.* **1997**, *40*, 4396−4405.

(20) Sauer, R.; Maurinsh, J.; Reith, U.; Fülle, F.; Klotz, K. N.; Müller, C. E. Water-soluble phosphate prodrugs of 1-propargyl-8-styrylxanthine derivatives, A2A-selective adenosine receptor antagonists. *J. Med. Chem.* **2000**, *43*, 440−448.

(21) Baraldi, P. G.; Cacciari, B.; Romagnoli, R.; Spalluto, G.; Monopoli, A.; Ongini, E.; Varani, K.; Borea, P. A. 7-Substituted 5-amino-2-(2-furyl)pyrazolo[4,3-*e*]-1,2,4-triazolo[1,5-*c*]pyrimidines as A2A adenosine receptor antagonists: a study on the importance of modifications at the side chain on the activity and solubility. *J. Med. Chem.* **2002**, *45*, 115−126.

(22) Matasi, J. J.; Caldwell, J. P.; Hao, J.; Neustadt, B.; Arik, L.; Foster, C. J.; Lachowicz, J.; Tulshian, D. B. The discovery and synthesis of novel adenosine receptor (A_{2A}) antagonists. *Bioorg. Med. Chem. Lett.* **2005**, *15*, 1333−1336.

(23) Vu, C. B.; Peng, B.; Kumaravel, G.; Smits, G.; Jin, X.; Phadke, D.; Engber, T.; Huang, C.; Reilly, J.; Tam, S.; Grant, D.; Hetu, G.; Chen, L.; Zhang, J.; Petter, R. C. Piperazine derivatives of [1,2,4]triazolo-

[1,5-a][1,3,5] triazine as potent and selective adenosine A2A receptor antagonists. *J. Med. Chem.* **2004**, *47*, 4291−4299.
(24) Vu, C. B.; Shields, P.; Peng, B.; Kumaravel, G.; Jin, X.; Phadke, D.; Wang, J.; Engber, T.; Ayyub, E.; Petter, R. C. Triamino derivatives of triazolotriazine and triazolopyrimidine as adenosine A2a receptor antagonists. *Bioorg. Med. Chem. Lett.* **2004**, *14*, 4835−4838.
(25) Jacobson, K. A.; Knutsen, L. P1 and P2 purine and pyrimidine receptor ligands. *Handbk. Exp. Pharmacol.* **2001**, *115*, 1129−1175.
(26) Jacobson, K. A.; IJzerman, A. P.; Linden, J. 1,3-Dialkylxanthine derivatives having high potency as antagonists at human A(2B) adenosine receptors. *Drug Dev. Res.* **1999**, *47*, 45−53.
(27) Kim, Y. C.; Karton, Y.; Ji, X. D.**;** Melman, N.; Linden, J.**;** Jacobson, K. A. Acylhydrazide derivatives of a xanthine carboxylic congener (XCC) as selective antagonists at human A2B adenosine receptors. *Drug Dev. Res.* **1999**, *47*, 178−188.
(28) Kim, Y. C.; Ji, X. D.; Melman, N.; Linden, J.; Jacobson, K. A. Anilide derivatives of an 8-phenylxanthine carboxylic congener are highly potent and selective antagonists at human A2B adenosine receptors. *J. Med. Chem.* **2000**, *43*, 1165−1172.
(29) Hayallah, A. M.; Sandoval-Ramirez, J.; Reith, U.; Schobert, U.; Preiss, B.; Schumacher, B.; Daly, J. W.; Müller, C. E. 1,8-Disubstituted xanthine derivatives: synthesis of potent A2B selective adenosine receptor antagonists. *J. Med. Chem.* **2002**, *45*, 1500−1510.
(30) Kim, S. A.; Marshall, M. A.; Melman, N.; Kim, S. H.; Müller, C. E.; Linden, J.; Jacobson, K. A. Structure-activity relationships at human and rat adenosine receptors of xanthine derivatives substituted at the 1-, 3-, 7-, and 8-positions. *J. Med. Chem.* **2002**, *45*, 2131−2138.
(31) Baraldi, P. G.; Tabrizi, M. A.; Preti, D.; Bovero, A.; Romagnoli, R.; Fruttarolo, F.; Zaid, N. A.; Moorman, A. R.; Varani, K.; Gessi, S.; Merighi, S.; Borea, P. A. Design, synthesis, and biological evaluation of new 8-heterocyclic xanthine derivatives as highly potent and selective human A2B adenosine receptor antagonists. *J. Med. Chem.* **2004**, *47*, 1434−1447.
(32) Castelhano, A. L.; Mckibben, B.; Witter, D. J. New N-6 substituted 7-deazapurine compounds active as inhibitors of A_1 adenosine receptor, useful for treating e.g. cognitive disease, renal failure, cardiac arrhythmia, ulcers, asthma, obstructive pulmonary disease or allergic rhinitis. U.S. 2002058667.
(33) Pastorin, G.; Ros, T. D.; Spalluto, G.; Deflorian, F.; Moro, S.; Cacciari, B.; Baraldi, P. G.; Gessi, S.; Varani, K.; Borea, P. A. Pyrazolo[4,3-*e*]-1,2,4-triazolo[1,5-*c*]pyrimidine derivatives as adenosine receptor antagonists. Influence of the N5 substituent on the affinity at the human A_3 and A2B adenosine receptor subtypes: a molecular modeling investigation. *J. Med. Chem.* **2003**, *46*, 4287−4296.
(34) Stewart, M.; Steinig, A. G.; Ma, C.; Song, J. P.; McKibben, B.; Castelhano, A. L.; MacLennan, S. J. [^{3}H]OSIP339391, a selective, novel, and high affinity antagonist radioligand for adenosine A2B receptors. *Biochem. Pharmacol.* **2004**, *68*, 305−312.
(35) (a) *Catalyst, version 4.10*; Accelrys Inc.: San Diego, U.S.A., 2005. (b) Catalyst 4.10 Tutorials. http://www.accelrys.com/doc/pdf/index.html (accessed month year).
(36) Catalyst Service on the Web. http://www.accelrys.com/products/catalyst/refs.html (accessed month year).
(37) Smellie, A.; Teig, S. L.; Towbin, P.; Poling: promoting conformational variation. *J. Comput. Chem.* **1995**, *16*, 171−187.
(38) Baraldi, P. G.; Cacciari, B.; Romagnoli, R.; Spalluto, G.; Moro, S.; Klotz, K. N.; Leung, E.; Varani, K.; Gessi, S.; Merighi, S.; Borea, P. A. Pyrazolo[4,3-*e*]1,2,4-triazolo[1,5-*c*]pyrimidine derivatives as highly potent and selective human A_3 adenosine receptor antagonists: influence of the chain at the N8 pyrazole nitrogen. *J. Med. Chem.* **2000**, *43*, 4768−4780.
(39) Peng, H.; Kumaravel, G.; Yao, G.; Sha, L.; Wang, J.; Vlijmen, H. V.; Bohnert, T.; Huang, C.; Vu, C. B.; Ensinger, C. L.; Chang, H.; Engber, T. M.; Whalley, E. T.; Petter, R. C. Novel bicyclic piperazine derivatives of triazolotriazine and triazolopyrimidines as highly potent and selective adenosine A2A receptor antagonists. *J. Med. Chem.* **2004**, *47*, 6218−6229.
(40) Zablocki, J.; Kalla, R.; Perry, T.; Palle, V.; Varkhedkar, V.; Xiao, D.; Piscopio, A.; Maa, T.; Gimbel, A.; Hao, J.; Chu, N.; Leung, K. and Zeng, D. The discovery of a selective, high affinity A2B adenosine receptor antagonist for the potential treatment of asthma. *Bioorg. Med. Chem. Lett.* **2005**, *15*, 609−612.
(41) Ilaš, J.; Pečar, S.; Hockemeyer, J.; Euler, H.; Kirfel, A.; Müller, C. E. Development of spin-labeled probes for adenosine receptors. *J. Med. Chem.* **2005**, *48*, 2108−2114.
(42) Feoktistov, I.; Blaggioni, I. Adenosine A2B receptors. *Pharmacol. Rev.* **1997**, *49*, 381−402.
(43) Chang, L. C. W.; Spanjersberg, R. F.; von Frijtag Drabbe Künzel, J. K.; Mulder-Krieger, T.; van den Hout, G.; Beukers, M. W.; Brussee, J.; IJzerman, A. P. 2,4,6-Trisubstituted pyrimidines as a new class of selective adenosine A_1 receptor antagonists. *J. Med. Chem.* **2004**, *47*, 6529−6540.
(44) Okamura, T.; Kurogi, Y.; Nishikawa, H.; Hashimoto, K.; Fujiwara, H.; Nagao, Y. 1,2,4-Triazolo[5,1-*i*]purine derivatives as highly potent and selective human adenosine A_3 receptor ligands. *J. Med. Chem.* **2002**, *45*, 3703−3708.
(45) Baraldi, P. G.; Preti, D.; Tabrizi, M. A.; Fruttarolo, F.; Romagnoli, R.; Zaid, N. A.; Moorman, A. R.; Merighi, S.; Varani, K.; Borea, P. A. New pyrrolo[2,1-*f*]purine-2,4-dione and imidazo[2,1-*f*]purine-2,4-dione derivatives as potent and selective human A_3 adenosine receptor antagonists. *J. Med. Chem.* **2005**, *48*, 4697−4701.
(46) Baraldi, P. G.; Tabrizi, M. A.; Preti, D.; Bovero, A.; Fruttarolo, F.; Romagnoli, R.; Zaid, N. A.; Moorman, A. R.; Varani, K.; Borea, P. A. New 2-Arylpyrazolo[4,3-*c*]quinoline derivatives as potent and selective human A_3 adenosine receptor antagonists. *J. Med. Chem.* **2005**, *48*, 5001−5008.
(47) Saki, M.; Tsumuki, H.; Nonaka, H.; Shimada, J.; Ichimura, M. KF26777 (2-(4-bromophenyl)-7,8-dihydro-4-propyl-1Himidazo[2,1-i]purin-5(4H)-one dihydrochloride), a new potent and selective adenosine A_3 receptor antagonist. *Eur. J. Pharmacol.* **2002**, *444*, 133−141.
(48) Minetti, P.; Tinti, M. O.; Carminati, P.; Castorina, M.; Cesare, M. A. D.; Serio, S. D.; Gallo, G.; Ghirardi, O.; Giorgi, F.; Giorgi, L.; Piersanti, G.; Bartoccini, F.; Tarzia, G. 2-*n*-Butyl-9-methyl-8-[1,2,3]-triazol-2-yl-9*H*-purin-6-ylamine and analogues as A_{2A} adenosine receptor antagonists. Design, synthesis, and pharmacological characterization. *J. Med. Chem.* **2005**, *48*, 6887−6896.
(49) (a) For merge hypotheses related information. http://www.accelrys.com/reference/cases/studies/CCKB_Pep_full.html (accessed month year). (b) Barreca, M. L.; Rao A.; Luca D. L; Zappala M.; Monforte A.-M.; Maga G.; Pannecouque C. et al. Computational Atrategies in Discovering Novel Non-nucleoside Inhibitors of HIV-1 RT. *J. Med. Chem.* **2005**, *48*, 3433−3437.
(50) During best fit analysis, mapping patterns of all conformers for each compound have been checked and statistically summarized. Our result shows that the mapping patterns given in Tables 4 and 7 with the best fit value are predominant among all conformer mapping patterns.
(51) Sauer, R.; Maurinsh, J.; Reith, U.; Fulle, F.; Klotz, KN.; Müller, C. E. Water-soluble phosphate prodrugs of 1-propargyl-8-styrylxanthine derivatives, A_{2A}-selective adenosine receptor antagonists. *J. Med. Chem.* **2000**, *43* (3), 440−448.

CI600410M